Nuclear induced breakup of halo nuclei

H. Esbensen
Physics Division, Argonne National Laboratory, Argonne, Illinois 60439

G. F. Bertsch
Institute for Nuclear Theory, University of Washington, Seattle, Washington 98195
(Received 13 January 1999)

We investigate the validity of approximations that are sometimes made in calculating the nuclear induced breakup of halo nuclei. We find that a truncated coupled-channels calculations, in which the nuclear couplings between continuum states are ignored, gives almost the same result as a first-order calculation. However, the couplings are much too strong to justify these approximations. This is demonstrated in the frozen limit of a semiclassical description, where one can compare to exact results. We find in this limit that the one-neutron removal cross section of ^{11}Be obtained in the approximate treatment is much larger than the exact result. This trend is also indicated at low energy by comparing a perturbative calculation of the breakup of ^{8}B to the result of a more realistic treatment, which evolves the wave function of the valence proton essentially to all orders in the target fields. [S0556-2813(99)01406-5]

PACS number(s): 24.10.−i, 25.60.−t

I. INTRODUCTION

In analyzing nuclear reaction cross sections of halo nuclei, the approximations that are commonly employed for tightly bound nuclei may become unreliable. For example, Al-Khalili *et al.* [1] have recently pointed out that the total reaction probability cannot be calculated to the needed accuracy by the commonly employed folded optical potential. In this paper we discuss the limitations of some of these approximations and point out why they fail.

The analysis is by far simplest at high beam energies, where the eikonal approximation can be used. Then all cross sections can be expressed in terms of probabilities calculated at fixed impact parameter, with the probabilities expressible as simple integrals over the trajectories. We shall study various approximations and compare their predictions in the frozen limit, where one ignores the effect of finite excitation energies.

The description of breakup reactions at low beam energies is much more difficult because one cannot ignore the finite excitation energies. Some authors have adopted a coupled-channels approach, which is the conventional method used to describe low-energy, heavy-ion reactions of ordinary nuclei. For halo nuclei, this requires a discretization of continuum states [2–4]. One approach is the method of coupled discretized continuum channels (CDCC), which was developed in the 1970s in light-ion studies; see Ref. [2] for a review. It was realized that the couplings among continuum states, as, for example, in deuteron breakup reactions, have a strong influence on the calculated results. However, such continuum-continuum couplings were completely neglected in recent studies [4] of the breakup of halo nuclei.

We will demonstrate that it is unrealistic to ignore continuum-continuum couplings when dealing with halo nuclei. This is most easily done at higher beam energies where the eikonal approximation is reliable. To test the approximation at low energies, we have also performed dynamical calculations, where we follow the time evolution of the halo wave function essentially to all orders in the fields from the target.

II. EIKONAL THEORY

We consider a halo nucleus interacting with the nuclear potential of a target nucleus. We adopt a semiclassical description, assuming that the projectile-target center of mass motion is given by a classical trajectory $\mathbf{r}(t)$. We can then focus on the quantal description of the relative motion of a halo nucleon and the core in the field from the target. Let us assume for simplicity that the halo-core Hamiltonian has only one bound state, the ground state $|0\rangle$, so that all excited states $|k\rangle$ belong to the continuum. In this section we also assume that the collision time τ is so short that the effect of finite excitation energies of the halo, ΔE_x, can be ignored during the collision, i.e., $\tau \Delta E_x \rightarrow 0$. We refer to this approximation as the frozen limit. The effect of interactions with the target on the halo state can then be calculated in the eikonal approximation, which provides the exact solution in this limit.

In the eikonal theory cross sections are expressed as integrals over impact parameter b of reaction probabilities $P(b)$, $\sigma = 2\pi \int b db P(b)$. The probabilities are extracted from the eikonal wave function, given by $\exp(i\chi)|0\rangle$, where χ is the eikonal phase. It depends on all the coordinates, but we will only treat the halo nucleon and the core explicitly, $\chi = \chi_n + \chi_c$. The eikonal phase will be calculated from the target optical potentials U_{nt} and U_{ct} (acting on the halo nucleon and the core, respectively) as

$$\chi(\mathbf{b}, \mathbf{r}_{nc}) = \frac{-1}{\hbar} \int_{-\infty}^{\infty} dt \ \{U_{nt}[\mathbf{r}(t) - \mathbf{r}_n] + U_{ct}[\mathbf{r}(t) - \mathbf{r}_c]\}. \tag{1}$$

It depends on the relative position of the halo nucleon and the core, $\mathbf{r}_{nc} = \mathbf{r}_n - \mathbf{r}_c$, i.e., $\mathbf{r}_n = \mathbf{r}_{nc}(1 - 1/A)$ and $\mathbf{r}_c =$

$-\mathbf{r}_{nc}/A$, where A is the mass number of the halo nucleus. The dependence on the trajectory is indicated by the impact parameter b.

A number of cross sections are measured in halo nucleus reactions. Very important is the total reaction cross section σ_R, associated with the probability

$$P_R = 1 - |a_0|^2, \tag{2}$$

where a_0 is the final amplitude of the ground state,

$$a_0 = \langle 0|e^{i\chi}|0\rangle. \tag{3}$$

For halo nuclei with a single bound state, two other cross sections can be measured. The diffraction dissociation cross section is the cross section that the nucleus breaks up, leaving the halo nucleon in a continuum state and the core intact. Here we need the amplitudes a_k for populating a continuum state $|k\rangle$. The full expression in the frozen limit is [5]

$$a_k = \langle k|e^{i\chi} - 1|0\rangle, \tag{4}$$

from which one obtains the diffraction dissociation probability

$$P_{\rm diff} = \sum_k |a_k|^2 = \langle 0| \ |e^{i\chi} - 1|^2 \ |0\rangle - |\langle 0|e^{i\chi} - 1|0\rangle|^2. \tag{5}$$

Another cross section is the so-called stripping cross section which is calculated from the halo stripping probability

$$P_{\rm str}(b) = \langle 0| \ |e^{i\chi_c}|^2 (1 - |e^{i\chi_n}|^2) \ |0\rangle. \tag{6}$$

It is determined by the imaginary parts of the eikonal phases and represents the probability that the halo nucleon is absorbed whereas the core fragment remains intact. Finally, the total one-nucleon removal cross section, which requires only that the core be left intact, is the sum of the stripping and the diffraction cross sections. The probability for this is

$$\begin{aligned} P_{-n}(b) &= P_{\rm str}(b) + P_{\rm diff}(b) \\ &= \langle 0| \ |e^{i\chi_c}|^2 \ |0\rangle - |\langle 0|e^{i(\chi_c + \chi_n)}|0\rangle|^2. \end{aligned} \tag{7}$$

III. FURTHER APPROXIMATIONS

The basic problem is to find a reliable way to treat χ. It is an ordinary function in the coordinate space representation but a nontrivial matrix in any other representation. The most drastic approximation is to keep only the ground-state to ground-state matrix element in χ,

$$\chi_0(b) = \langle 0|\chi(\mathbf{b}, \mathbf{r}_{nc})|0\rangle, \tag{8}$$

which is exponentiated to get the ground-state amplitude

$$a_0 = e^{i\chi_0}. \tag{9}$$

We shall refer to this approximation as the folding model because the eikonal phase is here determined by the total interaction being folded with the ground state density of the halo. This would be a reasonable approximation if $\chi = \chi_n + \chi_c$ were small or a slowly varying function of $\mathbf{r}_{nc}$. The part that is determined by the core-target interaction, χ_c, may fulfill the latter condition because $\mathbf{r}_c = -\mathbf{r}_{nc}/A$; so the dependence on $\mathbf{r}_{nc}$ is reduced by the total mass number A of the halo nucleus. The part that is determined by the halo-target interaction, χ_n, is more critical.

The eikonal phase χ_n is large inside the target nucleus and it is small only in the tail of the target field. The approximation (9) may therefore be reasonable for distant collisions of tightly bound nuclei in which the density overlap is small. When one of the colliding nuclei is a halo nucleus, on the other hand, some part of the extended halo will be traversed by the target nucleus and it will feel the much stronger part of the target field. This situation is best described by Eq. (3) whereas Eq. (9) is a poor approximation. An extreme view is the black disk approximation which is sometimes used to illustrate characteristic features of reactions with halo nuclei [6]. Thus, if the imaginary part of the nucleon-target interaction goes to infinity inside the target, the amplitude (9) would go to zero but the amplitude (3) would approach $a_0 \approx 1 - \nu$, where ν is the fraction of the halo density that is traversed by the target.

Al-Khalili *et al.* [1] found it necessary to use the full eikonal expression (3) rather than the folding model expression (9) to calculate the reaction probability P_R. Their analysis of high-energy experiments showed that total reaction cross sections of halo nuclei are typical 5–10 % larger in the folding model than those obtained from the full eikonal expression. This difference translates into an even larger difference between the rms radii that can be extracted from the data. Similar discrepancies between the reaction cross sections of ^{11}Li, calculated from the eikonal expression (3) and the folding model (9), have actually been noted earlier [7,8]. The nuclear part of these cross sections are compared in Fig. 3 of Ref. [7] and Table 3 of Ref. [8].

If χ is small, one can expand the exponentials in Eq. (5) and obtain the result of first-order perturbation theory. If the absorption is significant, it may be better to make an expansion in $(\chi - \chi_0)$, where χ_0 is defined in Eq. (8). This leads to the improved first-order expression

$$P^{(1)}_{\rm diff} = \langle 0| \ |\chi - \chi_0|^2 \ |0\rangle e^{-2\,{\rm Im}(\chi_0)}, \tag{10}$$

which is proportional to the mean-square fluctuation of χ in the halo ground state. It represents the semiclassical analog of the distorted wave Born approximation (DWBA) in the frozen limit.

IV. COUPLED-CHANNELS APPROACH

In the coupled-channels approach, one solves the set of coupled equations

$$\begin{aligned} i\hbar \frac{da_0}{dt} &= \langle 0|U|0\rangle a_0 + \sum_k \langle 0|U|k\rangle a_k e^{-i\omega_{k0}t}, \\ i\hbar \frac{da_k}{dt} &= \langle k|U|0\rangle a_0 e^{i\omega_{k0}t} + \sum_{k'} \langle k|U|k'\rangle a_{k'} e^{i\omega_{kk'}t}, \end{aligned} \tag{11}$$

where $U = U_{nt} + U_{ct}$ is the total interaction, and $\hbar\omega_{kk'}$ is the energy difference between the states considered. Note that

the complete solution to these equations reduces to the simple amplitudes (3) and (4) in the frozen limit, where the $\hbar\omega$'s are set to zero.

If we ignore all continuum-continuum couplings, and also the diagonal ground-state interaction, the coupled equations (11) reduce to the following form in the frozen limit:

$$i\hbar\frac{da_0}{dt}=\sum_k\langle 0|U|k\rangle a_k,\quad i\hbar\frac{da_k}{dt}=\langle k|U|0\rangle a_0. \tag{12}$$

The exact solutions to these equations can be derived from the expressions (3) and (4) simply by expanding $e^{i\chi}$ in powers of χ. All one has to realize is that the phase shift operator χ, according to Eq. (12), is only allowed to connect the ground state to continuum states and vice versa. The ground-state amplitude one thus obtains is

$$a_0=\sum_{n=0}^{\infty}\frac{(-\delta\chi^2)^n}{(2n)!}=\cos(\delta\chi), \tag{13}$$

where

$$\delta\chi^2=\sum_k\langle 0|\chi|k\rangle\langle k|\chi|0\rangle=\langle 0|\chi^2|0\rangle-\langle 0|\chi|0r\rangle^2. \tag{14}$$

Note that $\delta\chi^2$ and $\delta\chi$ can both be complex quantities.

One might want to keep some effect of the diagonal couplings. This can be done for example by assuming that $\langle k|U|k\rangle=\langle 0|U|0\rangle$ for all channels. The effect would then be an overall factor $e^{i\chi_0}$ on all amplitudes. Including this factor one obtains, for the total reaction probability,

$$P_R^{(\mathrm{tcc})}=1-|\cos(\delta\chi)|^2\ \exp[-2\ \mathrm{Im}(\chi_0)]. \tag{15}$$

The amplitudes for populating continuum states will be determined by odd powers of χ, and one obtains, similarly,

$$a_k=i\langle k|\chi|0\rangle\sum_{n=0}^{\infty}\frac{(-\delta\chi^2)^n}{(2n+1)!}=i\langle k|\chi|0\rangle\frac{\sin(\delta\chi)}{\delta\chi}. \tag{16}$$

Including again a common diagonal matrix element χ_0 one obtains the following expression for the elastic breakup probability:

$$P_{\mathrm{diff}}^{(\mathrm{tcc})}=(\langle 0|\ |\chi|^2\ |0\rangle-|\langle 0|\chi|0\rangle|^2)\left|\frac{\sin(\delta\chi)}{\delta\chi}\right|^2\times\exp[-2\ \mathrm{Im}(\chi_0)]. \tag{17}$$

This is the result one obtains in the frozen limit from the truncated coupled-channels (tcc) treatment used in Ref. [4]. It reduces to the first-order expression (10) when $\delta\chi$ is small.

V. COMPARISONS IN THE FROZEN LIMIT

Let us now compare the numerical results that one obtains in the frozen limit from the different approaches and choose the $^{11}\mathrm{Be}\rightarrow{}^{10}\mathrm{Be}+n$ nuclear induced breakup on a light target as an example. The valence neutron is bound by 0.5 MeV and the ground-state wave function can be determined from a Woods-Saxon well with depth 51.5 MeV, a radius of 3 fm, and a diffuseness of 0.52 fm.

The neutron interaction with the target is also simulated by a Woods-Saxon potential, with radius $R_{nt}=3$ fm, diffuseness $a_{nt}=0.69$ fm, and optical potential depth U_0+iW_0 with numerical values discussed below. Assuming a straight-line trajectory for the relative motion, $\mathbf{r}(t)=\mathbf{b}+\mathbf{v}t$, the eikonal phase is

$$\chi_n(\mathbf{b}-\mathbf{r}_{n\perp})=\chi_n^{(0)}\int_{-\infty}^{\infty}\frac{dz}{R_{nt}}\{1+\exp[(r-R_{nt})/a_{nt}]\}^{-1}, \tag{18}$$

where $r=\sqrt{(\mathbf{b}-\mathbf{r}_{n\perp})^2+z^2}$ is the distance between the valence neutron and the target, and the strength parameter $\chi_n^{(0)}$ is defined as

$$\chi_n^{(0)}=-\frac{U_0+iW_0}{\hbar v}R_{nt}. \tag{18a}$$

We have defined the strength parameter in this way to make clearer the magnitude of the controlling parameter in the approximations. It corresponds to the phase associated with a deeply penetrating neutron trajectory since the integral in Eq. (18) has a value between zero and roughly two.

We will consider three examples, two at lower energy, with a real and a complex neutron-target interaction, respectively, and one relevant to high-energy experiments, with a purely imaginary interaction. For the two lower-energy cases we take the velocity v in Eq. (18a) corresponding to a beam energy of 60 MeV/nucleon and a typical potential depth of $U_0=40$ MeV. This yields $\chi_n^{(0)}=1.8$, showing immediately that a perturbative treatment is invalid when penetrating neutron trajectories are significant. We also consider the effect of the absorptive part of the neutron-target interaction. At beam energies of 40–60 MeV/nucleon, the imaginary part of the potential is typically 1/3 of the real part, and we therefore consider the complex strength $\chi_n^{(0)}=1.8+0.6i$. At high energies, the real part of the interaction is small and the imaginary eikonal phase is related to the nucleon-nucleon cross section σ_{nn} and the target density ρ_t by $\chi=(i/2)\sigma_{nn}\int\rho_t(r)dz$. For beam energies in the range of 250 MeV/nucleon, this gives the result $\chi_n^{(0)}\approx 0.6i$ for our small target, which we take as our last case.

The phase shift associated with the core-target interaction is calculated, for simplicity as it was done in Ref. [1], in the folding model approximation (8):

$$\chi_{0c}=\langle 0|\chi_c(\mathbf{b}-\mathbf{r}_{c\perp})|0\rangle, \tag{19}$$

where

$$\chi_c(\mathbf{b}-\mathbf{r}_{c\perp})=\int d\mathbf{r}'\ \rho_c(r')\ \chi_n(\mathbf{b}-\mathbf{r}_{c\perp}-\mathbf{r}'_{\perp}). \tag{19a}$$

The core density is here parametrized as $\rho_c(r)=\rho_0[1+\alpha(r/a)^2]\exp[-(R/a)^2]$, with $\alpha=0.61$ and $a=1.79$ fm, and it is normalized to reproduce the mass number of the ^{10}Be core. The phase shift χ_{0c} is implicitly contained in the expressions given in the previous sections, where it is part of the diagonal phase shift $\chi_0=\chi_{0c}+\chi_{0n}$. Note that χ_{0c} is proportional to the strength parameter $\chi_n^{(0)}$, according to the

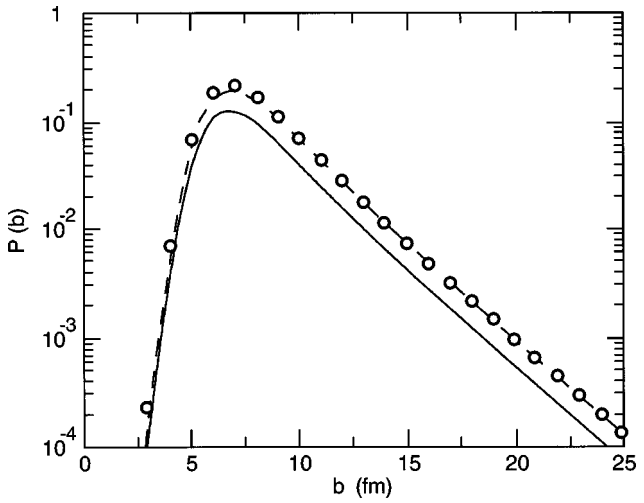

FIG. 1. Calculated diffraction dissociation probabilities for $^{11}\mathrm{Be}\rightarrow{}^{10}\mathrm{Be}+n$, as functions of the impact parameter, and obtained from a purely real neutron-target interaction as explained in the text. The solid curve is the result of the full eikonal expression, Eq. (5), the dashed curve is the result of the truncated coupled-channels approach, Eq. (17), and the open circles are the improved first-order results, Eq. (10).

construction (19), (19a). Note also that the cross sections discussed in the previous sections are sensitive only to the imaginary part of χ_{0c}. We shall therefore always adopt the strength $\chi_n^{(0)}=0.6i$ when calculating χ_{0c}.

The diffraction dissociation probabilities we obtain for the purely real eikonal phase, $\chi_n^{(0)}=1.8$, are illustrated in Fig. 1 as functions of impact parameter. It is seen that the perturbative result [open circles, Eq. (10)] is essentially identical to the truncated coupled-channels result [dashed curve, Eq. (17)], except for some deviation at smaller impact parameters. This is not surprising because the fraction $\nu(b)$ of the halo neutron that is penetrated by the target is quite small at the larger impact parameters. The quantity $\delta\chi^2$ defined in Eq. (14) is therefore dominated by the first term, which effectively is proportional to $\nu(b)$. From the explicit expression for the phase shift, Eq. (18), one can make the estimate

$$\delta\chi^2\sim\ \ \nu(b)\ \ (\chi_n^{(0)})^2. \tag{20}$$

Thus, when $\nu(b)$ is sufficiently small, $\delta\chi$ will also be small and Eq. (17) reduces to the perturbative result (10). Moreover, the same argument shows that the impact parameter dependence of these probabilities is also governed by $\nu(b)$ at larger b.

The solid curve in Fig. 1 is the exact result in the frozen limit, given by Eq. (5). It is also effectively proportional to the fraction $\nu(b)$ of the halo that is penetrated by the target, when $\nu(b)$ is small and the second term in Eq. (5) can be ignored. This explains why the exponential falloff in Fig. 1 is the same in all three cases. The dependence on the strength $\chi_n^{(0)}$ is, however, much more complicated for the exact result and the resulting dissociation probability is reduced to about 60% of the perturbative result.

It is interesting at this point to make contact to the scattering of free neutrons [9]. This can be done if we assume

TABLE I. Nuclear induced breakup cross sections for ^{11}Be, obtained in the frozen limit from the different reaction models discussed in the text, namely, the eikonal approximation, the truncated coupled-channels calculation (Tr. CCC), and the improved first-order calculation (Im. Pert. Th.). Results are shown for different phase shift strengths $\chi_{nt}^{(0)}$ associated with the neutron-target interaction. The contributions from stripping (σ_{str}) and diffraction dissociation (σ_{diff}) to the total one-neutron removal cross section (σ_{-n}) are shown, together with the total reaction cross section (σ_R), which includes a 1341 mb cross section from core absorption. The last line gives the results obtained from the folding model, Eqs. (8) and (9).

Model	$\chi_{nt}^{(0)}$	σ_{str} (mb)	σ_{diff} (mb)	σ_{-n} (mb)	σ_R (mb)
Eikonal	1.8	0	269	269	1610
Tr. CCC	1.8	0	432	432	1773
Im. Pert. Th.	1.8	-	462	-	-
Eikonal	$1.8+0.6i$	121	159	280	1621
Tr. CCC	$1.8+0.6i$	88	445	533	1875
Im. Pert. Th.	$1.8+0.6i$	-	471	-	-
Eikonal	$0.6i$	121	25	145	1487
Tr. CCC	$0.6i$	88	48	136	1477
Im. Pert. Th.	$0.6i$	-	47	-	-
Folding model	$0.6i$	-	-	183	1524

that the transverse density of the halo, $\rho_{h\perp}(b)$, is low and essentially constant over the target. We can then neglect the second term in Eq. (5) and estimate the first term by

$$P_{\mathrm{diff}}(b)\approx\rho_{h\perp}(b)\int d\mathbf{r}_\perp\ \ |e^{i\chi_n(r_\perp)}-1|^2. \tag{21}$$

Here we have also ignored the core-target interaction. The expression shows that the diffraction dissociation probability at large impact parameters is qualitatively governed by the transverse density of the halo and the diffractive scattering cross section of free neutrons. The assumption that the transverse density is constant is not realistic in practice. Thus the eikonal result shown in Fig. 1 is enhanced by 20% compared to the estimate (21).

Since the impact parameter dependence is mainly governed by $\nu(b)$ at larger b and core absorption at smaller b, it is sufficient just to compare the cross sections that one obtains in the different approaches. Results for different choices of the phase shift strength $\chi_n^{(0)}$ are shown in Table I. The choice $\chi_n^{(0)}=1.8+0.6i$ is probably the most realistic at 40–60 MeV/nucleon. In fact, the results we obtain in this case in the eikonal approach are in good agreement with the results shown in Fig. 2A of Ref. [5], at 40 MeV/nucleon on a light target. The truncated coupled-channels approach, on the other hand, gives a much larger one-neutron removal cross section, almost by a factor of 2.

The comparison may not seem so bad for a purely imaginary interaction, with $\chi_n^{(0)}=0.6i$; the one-neutron removal cross sections shown in Table I are almost identical in this case. However, the diffraction dissociation cross sections differ by almost a factor of 2. It is also noted that the perturba-

tive result is almost identical to the diffraction dissociation probability obtained in the truncated coupled-channels approach, for all three choices of $\chi_n^{(0)}$ shown in Table I. The above comparisons clearly show that neither the perturbative nor the truncated coupled-channels approach is reliable in describing the breakup of halo nuclei, at least when the frozen limit applies.

A purely imaginary neutron-target interaction is relevant to breakup reactions at very high energies, as employed in the work of Al-Khalili *et al.* [1]. In Table I we also quote in this case the one-neutron removal cross section and the total reaction cross section that we obtain from the folding model, Eqs. (8) and (9). They are about 40 mb larger than the results we obtain in the eikonal approximation. This difference is consistent with the results shown in Fig. 8 of Ref. [1], which confirms the interpretation given there, namely, that the folding model is unreliable when used to extract rms radii of halo nuclei from reaction data. Our reaction cross sections are larger than those given in Ref. [1]. That is caused by the fact that we have not fine-tuned the target interactions to be consistent with a high-energy experiment on a ^{12}C target. We refer to our earlier work [5], where we applied more realistic interactions and achieved good agreement with measurements using the eikonal approximation.

VI. DYNAMICAL CALCULATIONS

The description of breakup reactions of halo nuclei is much more difficult at low beam energies, and few experiments have been performed. One example is the ^{8}B breakup on a ^{58}Ni target at 26 MeV, which was measured at Notre Dame [10]. The breakup probability was found to be much smaller than expected from a calculation of the first-order $E1$ and $E2$ Coulomb dissociation.

Attempts to explain the small breakup probability have recently been made, based on the first-order DWBA [11] and on the truncated coupled-channels approach [4]. Both calculations showed that nuclear induced breakup plays a significant role in the vicinity of the kinematic region of the measurement. Moreover, they also showed that the commonly used multipole expansion of the Coulomb field from the target, which assumes that the distance from the ^{8}B projectile to the target is larger than the distance to the valence proton in ^{8}B, is not valid in this case. Both features are very unfortunate because they destroy the simple connection between electric multipole strength functions and breakup probabilities that is commonly used in first-order calculations; this makes the interpretation of the measurement much more difficult.

In order to test these theoretical results, we have performed a dynamical calculation, where we followed the time evolution of the valence proton wave function, essentially to all orders in the Coulomb and nuclear fields from the target. Our calculation is similar to those we performed at 46.5 MeV/nucleon on a Pb target [12]. There we used a straight-line trajectory and included the $E0$, $E1$, and $E2$ fields from the target. Here we use a Coulomb trajectory, and include in addition the associated nuclear multipole fields ($\lambda=0$, 1, and 2) from the proton-target interaction, whereas the nuclear core-target interaction is ignored. Our calculation may be considered an extension to higher orders of the first-order DWBA calculation reported by Nunes and Thompson [11], since we adopt the same proton-target interaction and include all angular momentum states up to $l=6$.

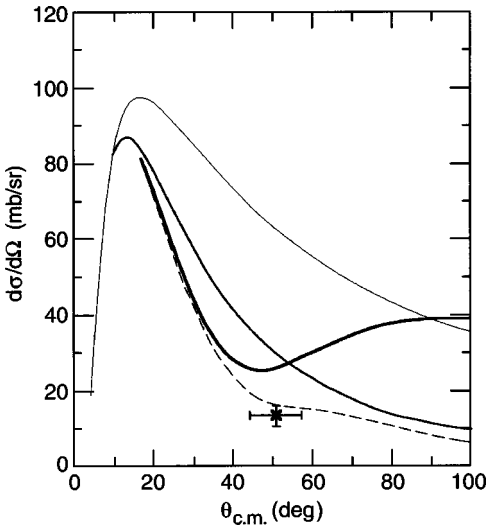

FIG. 2. Differential cross sections for the $^8\mathrm{B}\rightarrow{}^7\mathrm{Be}+p$ breakup at 26 MeV on a ^{58}Ni target, as functions of the ^{8}B center of mass scattering angle. The top thin curve is the result of the first-order Coulomb dissociation, obtained from the $E1$ and $E2$ strength distributions calculated in Ref. [12]. The next thicker curve is the result of a dynamical calculation, which includes the $E0$, $E1$, and $E2$ Coulomb fields to all orders. The thickest solid curve includes in addition the effect of the nuclear multipole fields ($\lambda=0$, 1, and 2) on the valence proton, and the dashed curve is the separate contribution from diffraction dissociation. The result of a measurement [10] is also shown.

The results of our calculations are shown in Fig. 2, as functions of the classical ^{8}B center of mass scattering angle. We also indicate our interpretation of the measurement [10] in terms of a differential cross section. It is seen that the first-order Coulomb dissociation (top thin curve), which is based on calculated $E1$ and $E2$ strength distributions [12], exceeds the measurement by almost a factor of 5. In the dynamical calculation, which includes the $E0$, $E1$, and $E2$ fields to all orders (the next thicker curve), the discrepancy with the measurement is reduced to a factor of 2.4. This reduction is partly caused by higher-order Coulomb processes but also by the fact that we here have used the correct multipole expansion of the Coulomb fields from the target which act both on the proton and on the ^{7}Be core.

The thickest solid curve in Fig. 2, which has a minimum near 48° and peak at large scattering angles, is the result we obtain when we also include the nuclear multipole fields ($\lambda=0-2$) from the target on the valence proton. The result is, to some extent, similar to the DWBA result (Fig. 3 of Ref. [11]) in the angular range below 50°. This confirms that the nuclear induced breakup does play an important role in the vicinity of the measurement. Our result has two contributions, from stripping and diffraction dissociation, and the dashed curve shows the separate contribution from diffraction dissociation.

While there is still some discrepancy with the measurement, maybe a factor of 2, we shall here focus on discrepan-

cies with the DWBA calculation. The main difference appears to be the magnitude of the peak at large scattering angles, which is a factor of 2 larger in the DWBA calculation. It is tempting to attribute this difference to the failure of first-order perturbation theory. This interpretation is in accordance with the comparisons made in the frozen limit in the previous section, where the discrepancy with the exact eikonal result was of similar magnitude. Thus it appears that, although the breakup probability is small, the nuclear field is way too strong to allow a perturbative treatment of the breakup of weakly bound nuclei, such as ^{8}B and ^{11}Be.

It is more difficult to compare to the truncated coupled-channels approach because the results that were published (see Fig. 10 of Ref. [4]) are limited to final state *s* waves. Anyway, even with this limitation on the final states, the calculated peak at large scattering angles has the same magnitude as our peak. In fact, from the comparison of results in the frozen limit presented in the previous section, we expect that a truncated coupled-channels calculation, in which one ignores the couplings between continuum states, should not differ much from a perturbative treatment.

VII. CONCLUSIONS

The picture that emerges from our investigation is that perturbation theory and also the coupled-channel approach that ignores continuum-continuum couplings are unreliable when it comes to a quantitative description of the nuclear induced breakup of halo nuclei. The two methods give similar results for diffraction dissociation; so not much is gained by solving the truncated set of coupled equations. Moreover, the breakup probabilities are often much larger (up to a factor of 2) than those obtained from other methods which are expected to be more reliable, namely, the eikonal approximation at high energies and the dynamical calculations at low energies.

The nuclear induced breakup may take place at large distances because of the extended nature of a halo, but the nuclear interaction of the halo nucleon with the target is much too strong to justify the perturbative or the truncated coupled-channels treatment.

This work was supported by the U.S. Department of Energy, Nuclear Physics Division, under Contracts No. W-31-109-ENG-38 and DE-FG-06-90ER-40561.

[1] J. S. Al-Khalili, J. A. Tostevin, and I. J. Thompson, Phys. Rev. C **54**, 1843 (1996).
[2] Y. Sakuragi, M. Yahiro, and M. Kamimura, Prog. Theor. Phys. Suppl. **89**, 136 (1986); Y. Hirabayashi and Y. Sukaragi, Phys. Rev. Lett. **69**, 1892 (1992).
[3] C. A. Bertulani and L. F. Canto, Nucl. Phys. **A539**, 309c (1992).
[4] C. H. Dasso, S. M. Lenzi, and A. Vitturi, Nucl. Phys. **A639**, 635 (1998); Phys. Rev. C **59**, 539 (1999).
[5] K. Hencken, G. F. Bertsch, and H. Esbensen, Phys. Rev. C **54**, 3043 (1996).
[6] P. G. Hansen, Phys. Rev. Lett. **77**, 1016 (1996).
[7] G. Bertsch, H. Esbensen, and A. Sustich, Phys. Rev. C **42**, 758 (1990).
[8] Y. Ogawa, K. Yabana, and Y. Suzuki, Nucl. Phys. **A543**, 722 (1992).
[9] S. Fernbach, R. Serber, and T. B. Taylor, Phys. Rev. **75**, 1352 (1949).
[10] Johannes von Schwarzenberg, J. J. Kolata, D. Peterson, P. Santi, M. Belbot, and J. D. Hinnefeld, Phys. Rev. C **53**, 2598 (1996).
[11] F. M. Nunes and I. J. Thompson, Phys. Rev. C **57**, 2818 (1998).
[12] H. Esbensen and G. F. Bertsch, Nucl. Phys. **A600**, 37 (1996).